

Characterization of Amino Hydroxamic Acids and Their Metal Chelates. Determination of Protonation and Formation Constants between 2-Amino-*N*-hydroxy-3-methylpentanamide and Copper(II), Nickel(II), Cobalt(II), and Hydrogen Ions in Aqueous Solution

Enrico LEPORATI

Istituto di Chimica Generale ed Inorganica dell'Università degli Studi di Parma,
Viale delle Scienze 78, 43100 - PARMA, Italy

(Received March 16, 1992)

The equilibria and relevant stability constant of species present in aqueous solutions of H^+ , Cu^{II} , Ni^{II} , and Co^{II} with "L - isoleucinehydroxamic acid" (2-amino-*N*-hydroxy-3-methyl pentanamide, ahmpe1) have been investigated by using potentiometric and spectrophotometric titrations at $25 \pm 0.1^\circ C$ and $I = 0.5 \text{ mol dm}^{-3}$ (KCl). The protonation constants of the ligand and the overall formation constants of several metal complexes were calculated from potentiometric and spectrophotometric data with the aid of the SUPERQUAD, and SQUAD programs, respectively. The following cumulative association constants (relative standard deviation values are given in parentheses) $\beta_{pqr} = [M_p H_q L_r] / [M]^p [H]^q [L]^r$ were obtained: $\log \beta_{011} = 9.15(1)$, $\log \beta_{021} = 16.40(1)$; Co^{II} -ahmpe1, $\log \beta_{111} = 12.26(1)$, $\log \beta_{101} = 5.50(1)$, $\log \beta_{102} = 9.46(6)$, $\log \beta_{1-11} = -1.71(2)$; Ni^{II} -ahmpe1, $\log \beta_{101} = 6.90(2)$, $\log \beta_{102} = 14.28(5)$, $\log \beta_{1-12} = 6.06(2)$; Cu^{II} -ahmpe1, $\log \beta_{101} = 10.36(1)$, $\log \beta_{102} = 19.85(1)$, $\log \beta_{2-12} = 20.90(1)$, $\log \beta_{1-12} = 10.29(1)$. The ligand is bound to the metal ions through the coordination of the N atoms of the α -amino and the deprotonated $-NHO^-$ groups. The UV-vis studies can be used to follow the appearance of the individual species, to estimate the coordination sphere around the metal ion and to observe the equilibria between different complexes. So the solution electronic spectra have been also employed to suppose a weak tetragonal coordination in the $[CuL_2(H_2O)_2]$ complex. Equilibrium constants for their formation and the probable structure of the chelated compound formed in aqueous solution are the object of discussions in terms of their possible significance to biological reactions, and their stability is compared with that of analogous chelated compounds.

Several studies have been recently carried out on hydroxamic acids and their metal complexes owing to the possible biological activity connected with these compounds. Many of the naturally occurring siderophores (low-molecular-weight compounds of microbial origin) use the hydroxamic acid functional groups for iron chelation and they act as growth factors, tumor inhibitors, constituents of antibiotics, cell-division growth factors, antibiotic antagonists, and pigments.^{1,2} Some of these compounds have showed themselves to be potent inhibitors of thermolysin, elastase, and aminopeptidase.³ Regarding the strong ability of this type of ligands to form chelates, the main question concerns the kind of donors of hydroxamic moiety ($-CONHOH$), i.e. nitrogen or oxygen, involved in the coordination to metal ion. However, when the hydroxamic acid contains also another donor, such as an amino group, the coordination could involve this group ($-NH_2$) as well as the nitrogen or the oxygen of the hydroxamic function. Even in the field of analytical chemistry amino hydroxamic acids have long had an important role, for example as analytical reagents for a variety of metal ions.⁴ Although a lot of work has been done on their synthesis and biological and structural characterization, relatively fewer papers have appeared dealing with the solution equilibria of proton and metal complexes of hydroxamic acids, and the amount of spectrophotometric studies done on these systems is very small.

Owing to the considerable interest in solution chemistry of hydroxamic acids and metal hydroxamates and

their biological role, a detailed potentiometric study of the equilibria of 2-amino-*N*-hydroxy-3-methylpentanamide (ahmpe1) with protons, Co^{2+} , Ni^{2+} , and Cu^{2+} was undertaken. The electronic spectra of the Cu^{2+} -system are also reported.

Experimental

Reagents. 2-Amino-*N*-hydroxy-3-methylpentanamide [(ahmpe1), L-isoleucinehydroxamic acid = HL] was obtained from Sigma (St. Louis, MO) and its purity and the exact concentration of its solution were checked by potentiometric titrations. Doubly distilled and deionized water was used in all potentiometric and spectrophotometric experiments and reagent grade chemicals were used without further purification. All other metal (chlorides, AnalaR Products) solutions were prepared and standardized by using standard analytical procedures.^{5,6} All titration solutions were prepared to have a total volume of $25.0 \pm 0.01 \text{ cm}^3$ and thermostatted at $25.0 \pm 0.1^\circ C$ with a Paratherm electronic (Julabo) circulating constant-temperature water bath. The accurate molarity of potassium hydroxide (ca. $0.4337 \text{ mol dm}^{-3}$) and hydrochloric acid ($0.4326 \text{ mol dm}^{-3}$) stock solutions were determined by conventional potentiometric titrations according to Gran's method, with the use of different calculation procedures as previously described.⁵⁻⁹ All these solutions were then raised to final total volume of 25.0 cm^3 by adding successively to the titration vessel a known volume of ahmpe1 solution and an exact volume of metal chloride; then, the required quantities of potassium chloride and a sufficient amount of doubly distilled water were added to make up the total volume V_0 .

Potentiometric Measurements. The equilibrium

studies were performed by using a Metrohm Titroprocessor E 636 instrument with a combined electrode 8102SC Ross (ORION Research). The system was calibrated in terms of hydrogen ion concentrations before and after a series of measurements by titrations of hydrochloric acid solution at $25.0 \pm 0.1^\circ\text{C}$ and $I = 0.5 \text{ mol dm}^{-3}$ (KCl) with a standard carbonate-free potassium hydroxide solution, according to Gran's method,⁸⁾ by using the computer programs NBAR⁹⁾ and MAGEC¹⁰⁾ as previously described. The solution in the titration compartment was shaken by means of a mechanical stirrer. A thermostatted stream of nitrogen, presaturated with water vapour by bubbling it through a 0.5 mol dm^{-3} KCl solution, was passed over the surface of the solution in the titration vessel. Small amounts ($\Delta v = 0.05$ or 0.025 cm^3) of titrant were added with the use of a Metrohm Dosimat E 635 autoburet (total volume = 5.0 cm^3). Emf readings for potentiometric experiments (*dynamic* and *monotonous*)¹¹⁾ and titration curves were recorded graphically by using an E 636 automatic titrator and a thermoprinter. The range of concentration of ligand in the potentiometric titrations was 0.0104 – $0.0124 \text{ mol dm}^{-3}$ for ahmpe1- H^+ (pH range 4.08–11.03; number of titrations 4); 0.0110 – $0.0121 \text{ mol dm}^{-3}$ for ahmpe1- Cu^{2+} (pH range 2.97–9.61; number of titrations 6); 0.0110 – $0.0121 \text{ mol dm}^{-3}$ for ahmpe1- Ni^{2+} (pH range 3.84–8.76; number of titrations 6); 0.0110 – $0.0142 \text{ mol dm}^{-3}$ for ahmpe1- Co^{2+} (pH range 3.85–9.23; number of titrations 6). The metal concentration varied between 0.00266 – $0.00708 \text{ mol dm}^{-3}$ for ahmpe1- Cu^{2+} ; 0.00306 – $0.00748 \text{ mol dm}^{-3}$ for ahmpe1- Ni^{2+} and 0.00305 – $0.00742 \text{ mol dm}^{-3}$ for ahmpe1- Co^{2+} systems, and potassium chloride ($I = 0.5 \text{ mol dm}^{-3}$) was used as supporting electrolyte.

Spectrophotometric Measurements. Absorption spectra in the ranges 400 – $820 \pm 0.3 \text{ nm}$ for Cu^{2+} -ahmpe1 system were measured with a KONTRON UVIKON 860 spectrophotometer to the fourth decimal place with a stepping of 2 nm . Solutions containing the ligand and the cupric ion prepared and maintained under purified nitrogen at the ionic strength 0.5 mol dm^{-3} (KCl), were measured at pH from 3.48 to 9.79 at $25.0 \pm 0.1^\circ\text{C}$ using 10 mm cells.

Calculations. Starting from several sets of potentiometric calibration (*dynamic* titration, where Δv of KOH added is inversely proportional to ΔE) data, first some parameters in acidic and alkaline solution (E° , A_j , B_j , v_e , and N) were refined simultaneously by using NBAR program, as reported in Table 1. In the present calculations some experimental points (v , E) around the equivalent point have been neglected. Successively, since the liquid-junction potentials (A_j and B_j) of the cell used in the measurements are fairly small, starting from the same potentiometric data, other parameters relating to calibration curves (E° , $2.303 RT/F$, K_w , and v_e) were calculated by applying the MAGEC program. Careful attention has been taken in the calculation and critical evaluation of the parameters relative to the potentiometric calibration curves, using different mathematical procedures as previously described.^{5–11)} In particular, by observing the results reported in Table 1 it is possible to verify the good agreement between the parameters (v_e and N) obtained from the two computer programs (maximum variation 0.6 and 0.5%, respectively). At the same time the differences of these parameters were non significantly from the mean values. Additionally, accurate examination of the results in Table 1 also reveals a good agreement in

the standard potential, E° , even if it is well-known that the standard potential of glass membrane is inclined to change day to day (owing to asymmetry effects) and that the liquid-junction potentials (A_j and B_j) don't repeat themselves easily, as can be seen from the calculations performed with the program NBAR. A more important factor that critically affects the refinement by the program MAGEC, is the value used for the dissociation constant of water, K_w , while in the calculations with the program NBAR, this parameter was kept constant ($K_w = 1.8450 \times 10^{-14}$). This parameter is very sensitive to correlations with the concentration of alkali in the burette. In those situations when K_w is uncertain, subprogram CALIBT (MAGEC program) permits the user to systematically vary the estimate of K_w . Thus the precision of the standard electrode potential, E° , and especially of the ionic product of water can be deduced only from the intertitration variability [all the points (acid and alkaline zones) in a single titration are considered]. In particular, values of K_w (Table 1) differ significantly from one experiment to another. Moreover it is generally accepted that E° can change with the passing of time, probably due to ageing of the electrode. Really the statistical analysis shows how the parameters (E°) obtained from the two regions (acidic and alkaline) of the same calibration curves and those from one titration to another are sometimes significantly different from the mean value or from them (E° in acidic and alkaline solution), thus showing that unexpected factors differing from one titration to another can alter the emf values and are the main source of error.

All the calculations were carried out on the CRAY Y-MP 432 and IBM 9377/90 computers of the Consorzio per la Gestione del Centro di Calcolo Elettronico Interuniversitario dell'Italia Nord Orientale, Casalecchio di Reno, Bologna, Italy, with the financial support of the University of Parma. Listings of the experimental data for the computations from SUPERQUAD,¹²⁾ NBAR, MAGEC, and SQUAD¹³⁾ programs are available as Supplementary Material and can be obtained on request to the author, upon full citation of the present article.

Results and Discussion

Protonation Equilibria. In the normal aqueous titration range a maximum number of two protons can be liberated from the ligand in the fully protonated form ($\text{Hahmpe1} = \text{H}_2\text{L}^+$) on titration with strong base in the pH range 4.08–11.03. Initially the overall protonation constants ($\log \beta_{011}$, and $\log \beta_{021}$) of the ligand and the initial amounts (mmol) of the reagents (T_H , T_L) were calculated at the same time through the refinement of several sets of potentiometric titration data, (number of experimental data points = 257, $\sigma = 0.32$, $\chi^2 = 11.61$) by SUPERQUAD without introducing the liquid-junction potentials into the calculations, as shown in earlier published papers.^{8–11)} The potentiometric titration curves [calculated (line) and observed (symbol)] of the completely protonated form of Hahmpe1 (H_2L^+) is shown in Fig. 1.

The ligand Hahmpe1 (Scheme 1) has two macroscopic protonation centres, the corresponding equilibria involving the terminal hydroxamate moiety (–

Table 1. Evaluation of the Equivalence Point, v_e/cm^3 , $N/\text{mol dm}^{-3}$ (Normality of KOH), K_w (Ionic Product of Water), E°/mV^a (Standard Potential), A_j/mV^a (Junction Potential in Acid Solution), B_j/mV^a (Junction Potential in Basic Solution), and $2.303 RT/F$ (Nernstian Slope) ^a from Eight Potentiometric Titrations of HCl ($0.43264 \text{ mol dm}^{-3}$) with KOH at 25°C and $I=0.5 \text{ mol dm}^{-3}$ (KCl) Using the Programs NBAR and MAGEC

Run	MAGEC					NBAR ^{b)}				
	E°	$2.303RT/F$	$10^{14}K_w$	v_e	$10^{14}K_w^{c)}$	E°	A_j	B_j	v_e	N
1 ^{d)}	400.50(7) ^{e)}	59.07(1) ^{e)}	1.8879 ^{e)}	2.395 ^{e)}	1.8827	401.29(8) ^{f)} 401.14(9) ^{g)}	-28.70(6.24) ^{f)} -10.93(4.21) ^{g)}		2.394 ^{f)} 2.393 ^{g)}	0.43380 ^{f)} 0.43396 ^{g)}
2	399.70(4)	59.11(1)	1.8793	1.999	1.8746	400.03(13) 400.29(8)	-26.64(36.28) -13.37(3.73)		1.993 1.994	0.43412 0.43384
3	399.90(10)	58.96(1)	1.8880	1.996	1.8879	401.40(9) 401.46(5)	-51.48(4.82) -35.50(2.37)		1.995 1.994	0.43382 0.43401
4	398.30(7)	58.78(1)	1.7539	1.996	1.7478	398.41(10) 399.80(6)	-54.21(10.42) 2.66(2.65)		1.994 1.993	0.43389 0.43409
5	396.90(6)	58.74(1)	1.7219	1.996	1.7222	398.03(9) 399.80(6)	-38.40(6.05) 2.44(4.19)		1.996 1.994	0.43344 0.43393
6	397.70(14)	59.10(1)	1.7298	1.996	1.7947	397.55(13) 398.26(10)	8.83(4.87) 48.09(5.13)		1.998 1.998	0.43305 0.43297
7	400.50(3)	59.12(1)	1.6827	1.996	1.6733	399.18(7) 401.69(10)	-24.27(5.43) -33.62(6.12)		1.994 1.993	0.43395 0.43425
8	399.60(5)	59.14(1)	1.7345	1.995	1.8703	399.38(8) 399.70(10)	-29.94(6.27) -14.16(4.86)		1.997 1.993	0.43335 0.43412

a) Standard deviations in E° , $2.303RT/F$, A_j , and B_j are given in parentheses. b) In the calculations, K_w was kept constant ($1.8937 \times 10^{-14} \text{ mol}^2 \text{ dm}^{-6}$). c) Parameter calculated from the experimental data in alkaline solution following the principles of Gran by keeping E° as obtained in acidic zone. d) Initial amount of hydrochloric acid was 2.4 cm^3 , for all the others 2.0 cm^3 . e) Using all the buffered data. f) Parameters calculated following the principles of Gran by using the experimental data in acidic solution. g) Parameters calculated following the principles of Gran by using the experimental data in alkaline solution.

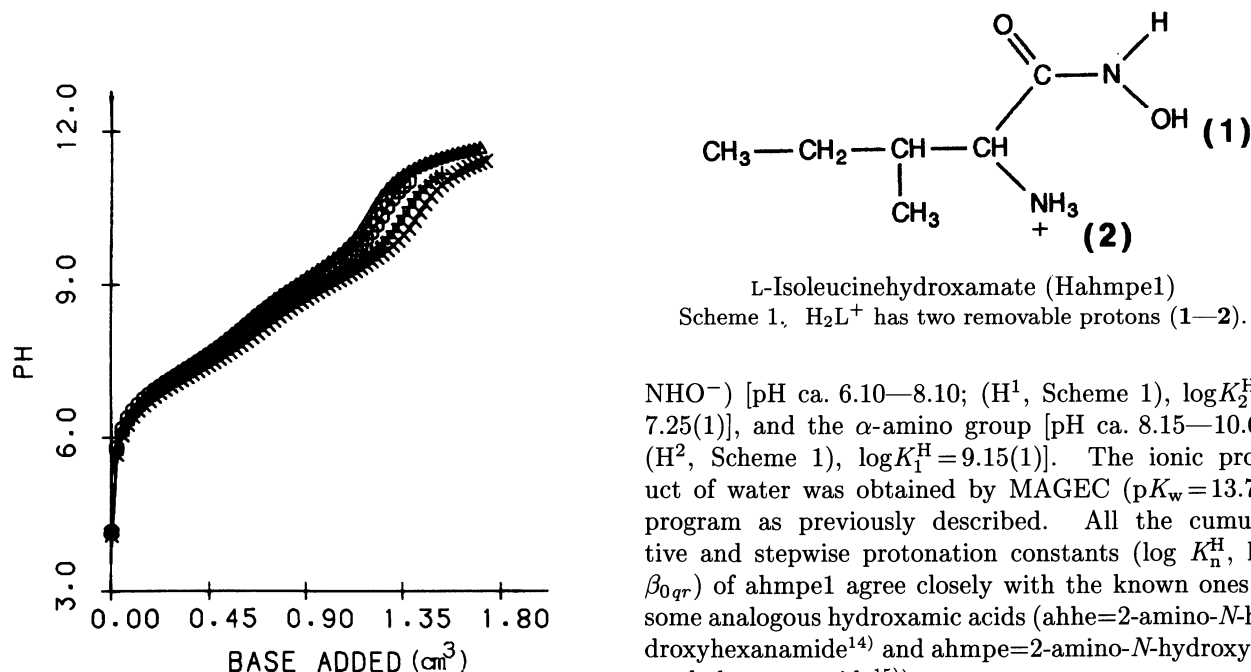


Fig. 1. Experimental and calculated (by SUPERQUAD program) titration curves of pH as a function of volume of KOH added for H^+ -ahmpel system, $V_0=25.0\text{ cm}^3$, $C_{KOH}=0.4338\text{ mol dm}^{-3}$ [T_L range 0.2607—0.3086, T_H range 0.5214—0.6175]. T_L and T_H are mmol of ahmpel and hydrogen ion in the titration vessel.

NHO⁻) [pH ca. 6.10—8.10; (H¹, Scheme 1), $\log K_2^H = 7.25(1)$], and the α -amino group [pH ca. 8.15—10.60; (H², Scheme 1), $\log K_1^H = 9.15(1)$]. The ionic product of water was obtained by MAGEC ($pK_w = 13.74$) program as previously described. All the cumulative and stepwise protonation constants ($\log K_n^H$, $\log \beta_{0qr}$) of ahmpel agree closely with the known ones of some analogous hydroxamic acids (ahhe=2-amino-*N*-hydroxyhexanamide¹⁴) and ahmpe=2-amino-*N*-hydroxy-4-methylpentanamide¹⁵).

Metal-Complex Equilibria. The existence of metal-proton-amino hydroxamic acid (ahmpel) complexes was examined using the values $p=1-3$, $q=1, 2, -1, -2$, and $r=1, 2, 3$. The equilibrium pattern was selected by successive attempts according to the best agreement between observed and calculated data and by means of an accurate statistical analysis of the following parameters: the agreement factor (σ^2), the

goodness of fit (χ^2), the standard deviation (σ) of the formation constants, and the chemical significance of the species proposed. At this point all the protonation constants were kept constant and the computer program SUPERQUAD was employed for a second stage of refinement in which emf data for solutions with various metal ion-ligand ratios were processed in order to investigate the binary systems. The calculated complex formation constants, $\log \beta_{pqr}$ for the ahmpel with different metals are given in Table 2.

Starting from the stability constants given in Table 2 and the protonation constants of ahmpel under the same experimental conditions, the percentage of each complex involving H^+ or OH^- , metal ion, and ligand has been calculated by using the HALTAFALL program with a Calcomp 936 Plotter Typical distribution diagram is shown in Fig. 2. The refinement converged satisfactorily when the only species present for ahmpel were $[CuL]^+$, $[Cu_2(OH)L_2]^+$, $[CuL_2]$, and $[Cu(OH)L_2]^-$; $[NiL]^+$, $[NiL_2]$, and $[Ni(OH)L_2]^-$; $[CoL]^+$, $[CoHL]^{2+}$, $[CoL_2]$, and $[Co(OH)L]$. In the case of Cu^{2+} -ahmpel system the complexation begins at pH ca. 3.0 with the formation of $[CuL]^+$ and the dimer $[Cu_2(OH)L_2]^+$ species, which reaches its maximum concentration of 89% at pH 4.4. Previous authors^{16,17} too have concluded that the dimer is in equilibrium with the mononuclear complex $[CuL]^+$, which is present in small quantity (maximum of 9.7 % at pH 3.75). The species

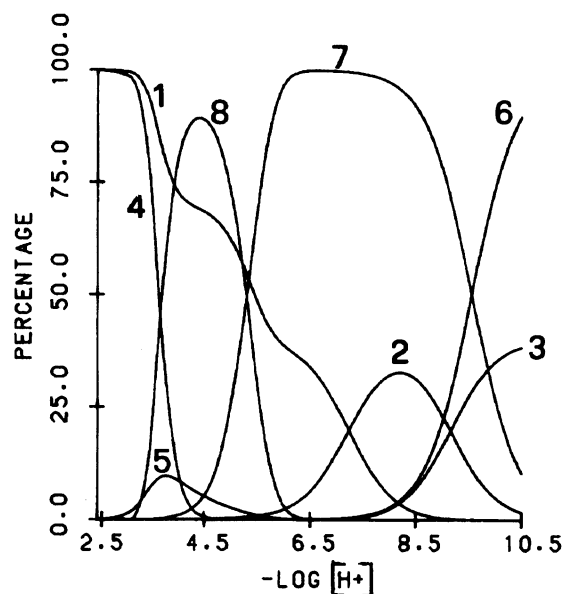


Fig. 2. Typical distribution diagram for Cu^{2+} -ahmpel system. The percentage of each species has been calculated from the data of a hypothetical solution of copper ions ($0.0033 \text{ mol dm}^{-3}$) and ahmpel ($0.011 \text{ mol dm}^{-3}$) by the HALTAFALL program (N. Ingri, W. Kakalowicz, L. G. Sill  n, and B. Warnqvist, 14, 1261 (1967)), and using a PLOTTER Calcomp 936. The percentages of the species not containing copper were calculated as percentages of the total ligand, those containing copper as percentages of the total metal. (1) H_2L^+ , (2) HL , (3) L^- , (4) Cu^{2+} , (5) CuL^+ , (6) $Cu(OH)L_2^-$, (7) CuL_2 , (8) $Cu_2(OH)L_2^+$.

Table 2. Cumulative and Stepwise Protonation Complex Formation Constants of 2-Amino-*N*-hydroxy-3-methylpentanamide (ahmpel) at 25°C and $I = 0.5 \text{ mol dm}^{-3}$ (KCl).

	SUPERQUAD			
	H^+	Co^{2+}	Ni^{2+}	Cu^{2+}
$\log \beta_{011}$	9.15(1)			
$\log \beta_{021}$	16.40(1)			
$\log K_2^{H^a}$	7.25(1) ^b			
$\log \beta_{111}$		12.26(1)		
$\log \beta_{101}$		5.50(1)	6.90(2)	10.36(1)
$\log \beta_{2-12}$				20.90(1)
$\log \beta_{1-12}$			6.06(2)	10.29(1)
$\log \beta_{102}$		9.46(6)	14.28(5)	19.85(1)
$\log \beta_{1-11}$		-1.71(2)		
Z^c	257	328	350	331
χ^2^d	11.61	11.41	14.43	9.57
U	2.52×10^1	1.14×10^3	1.80×10^3	1.48×10^3
σ^e	0.32	1.87	2.27	2.12

a) $\log K_n = \log \beta_{0n1} - \log \beta_{0n-11}$. b) $\sigma(\log K_n) = [(\sigma^2(\log \beta_{0n1}) + \sigma^2(\log \beta_{0n-11}))/2]^{1/2}$. c) Total number of experimental data points used in the refinement. d) Observed χ^2 ; Calculated value (6, 0.95) should be 12.6, where 6 is the number of degrees of freedom and 0.95 is the confidence coefficient in the χ^2 distribution.

e) $\sigma = \sqrt{\sum_{i=1}^Z w_i (E_i^{\text{obsd}} - E_i^{\text{calcd}})^2 / (Z - m)}$, where m is the number of parameters to be refined.

$[CuL_2]$ reaches a maximum concentration of 99.8% total copper at pH 6.75. The Cu^{2+} -ahmpel system showed two distinct buffer zones separated by a sharp equivalence point between them that would exactly correspond to a 1.25 molar ratio (mol of base added per two mol of metal ion). The complex $[ML]^+$ reaches a maximum concentration of 22.0 % total nickel at pH 5.75, 39.5 % total cobalt at pH 7.0 corresponding to the displacement of two protons. The species $[ML_2]$ reaches a maximum concentration of 96% total nickel at pH 6.75, 34% total cobalt at pH 8.2. Above pH 7.0, one hydrolyzed species was detected: The maximum fraction of the complex $[Cu(OH)L_2]^-$ is ca. 83% at pH 10.25; $[Ni(OH)L_2]^-$ has a maximum fraction of ca. 99% at pH 10.5, while $[Co(OH)L]$ reaches a peak of ca. 97% at pH 10.5. Typical absorption spectra for Cu^{2+} -ahmpel system are plotted in Fig. 3, in the pH range 3.48–9.79. At low pH a broad absorption spectrum is present and its maximum shifts towards visible region as the pH increases [maximum, 0.174 A at 718 nm(1); 0.256 A at 670 nm(2); 0.350 A at 656 nm(3); 0.448 A at 650 nm(4); 0.540 A at 646 nm(5); Fig. 3]. The first maximum of absorbance in the range 640–650 nm occurs at pH 4.104 and λ_{max} of 646 nm and corresponding ca. to the maximum concentration

Table 3. Comparison of the Absorption Maxima (nm) and the Isosbestic Points (nm) for $[\text{Cu}_2(\text{OH})\text{L}_2]^+$, $[\text{Cu}(\text{OH})\text{L}_2]^-$, and $[\text{CuL}_2(\text{H}_2\text{O})_2]$ hydroxamate-complexes. Parameters ($\epsilon/\text{dm}^3 \text{ mol}^{-1} \text{ cm}^{-1}$, ν/cm^{-1} , $\Delta\nu/\text{cm}^{-1}$) of the Component Bands Obtained from Gaussian Analysis of the Absorption Spectrum of $[\text{CuL}_2(\text{H}_2\text{O})_2]$ (L=isoleucinehydroxamate), f Values Refer to the Oscillator Strengths for the Transitions ^{a)}

Assignment [$\text{CuL}_2(\text{H}_2\text{O})_2$]	ϵ	ν	$\Delta\nu$	f
${}^2\text{B}_{1g} \rightarrow {}^2\text{A}_{1g}$	36.35	16 926.5	3 749.3	6.2692×10^{-4}
	29.908 ^{b)}	16 199.9	4 773.0	6.5667×10^{-4}
	27.38 ^{c)}	16 647.5	3 798.7	4.7844×10^{-4}
	29.29 ^{d)}	16 797.8	4 000.1	5.3900×10^{-4}
	34.26 ^{e)}	16 800.5	4 001.2	6.3052×10^{-4}
	53.71 ^{f)}	16 800.2	4 001.1	9.886×10^{-4}
	33.58 ^{g)}	16 799.2	4 147.8	6.404×10^{-4}
	25.734 ^{h)}	16 820.4	5 119.6	6.057×10^{-4}
${}^2\text{B}_{1g} \rightarrow {}^2\text{B}_{2g}$	51.96	18 939.4	3 943.1	9.4246×10^{-4}
	48.125 ^{b)}	18 199.9	4 282.5	9.4807×10^{-4}
	61.00 ^{c)}	18 451.4	3 996.9	1.1215×10^{-3}
	54.50 ^{d)}	18 492.7	4 378.5	1.0977×10^{-3}
	48.00 ^{e)}	18 501.4	4 374.6	9.6595×10^{-4}
	80.93 ^{f)}	18 500.2	4 374.9	1.629×10^{-3}
	48.11 ^{g)}	18 824.0	4 191.8	9.272×10^{-4}
	53.571 ^{h)}	18 382.3	4 861.7	1.197×10^{-3}
${}^2\text{B}_{1g} \rightarrow {}^2\text{E}_g$	36.72	21 048.8	5 202.5	8.7876×10^{-4}
	40.985 ^{b)}	21 550.1	5 661.5	1.067×10^{-3}
	44.62 ^{c)}	21 550.9	5 663.6	1.1625×10^{-3}
	35.26 ^{d)}	20 496.3	4 707.9	7.6397×10^{-4}
	36.10 ^{d)}	20 500.1	4 705.8	7.8149×10^{-4}
	48.46 ^{f)}	20 499.2	4 706.1	1.049×10^{-3}
	29.56 ^{g)}	20 517.7	5 066.8	6.855×10^{-4}
	42.472 ^{h)}	20 490.9	5 211.2	1.017×10^{-3}
Ligand	$[\text{Cu}_2(\text{OH})\text{L}_2]^+$	$[\text{Cu}(\text{OH})\text{L}_2]^-$	$[\text{CuL}_2(\text{H}_2\text{O})_2]$	Isosbestic point
ahmpe1	648 nm	530 nm	546 nm	587 nm
adhp ^{f)}	653	496	547	594
adhb ^{e)}	651	508	553	595
ahpr ^{d)}	648	518	540	593
ahmpe ^{b)}	648		549	589
aimahp ^{c)}	648	450	536	591
ahbt ^{l)}	647	538	562	602
ahmpe ^{h)}	649		530	595

a) Relative standard deviation (%) or coefficient of variation for Cu^{2+} -ahmpe1 system =0.34; region of spectrum 12195—25000 cm^{-1} . For abbreviations of the ligands see caption of Fig. 6. h) Ref. 18. g) Ref. 16.

(83%) of the hydrolyzed dimeric complex [see Fig. 2, curve 8]. The increase in absorption (*hyperchromic effect*) of the broad spectrum near the i.r. region and the shift towards smaller wavelengths (*hypsochromic effect*) of the same band with increasing pH indicates greater complexation, due to the appearance of the hydrolyzed binuclear species, $[\text{Cu}_2(\text{OH})\text{L}_2]^+$ (intense green color, maximum absorption at 646—650 nm). When the pH is increased further on from 4.26 to 9.79 (Fig. 3) combined *hyperchromic-hypochromic* and high *hypsochromic effects* [maximum, 0.517 A at 634 nm(6); 0.454 A at 568 nm(7); 0.524 A at 540 nm(8); 0.551 A at 534 nm(9);

0.547 A at 526 nm(10); Fig. 3] are observed (change of color from intense green to purple in acidic media), while for $\text{pH} > 5.2$ a simultaneous increase in the absorption (*hyperchromic shift*) and a small decrease in the wavelength (*hypsochromic effect*) [maximum, 0.454 A at 568 nm(7); 0.524 A at 540 nm(8); 0.551 A at 534 nm(9); 0.547 A at 526 nm(10); Fig. 3] occurs with the formation of the complexes $[\text{CuL}_2]$ (maximum absorption at 540—550 nm) and $[\text{Cu}(\text{OH})\text{L}_2]^-$. The color changes from purple to reddish purple. One distinctive isosbestic point appears at 587 nm [Fig. 3]. This corresponds to an equilibrium $[\text{Cu}_2(\text{OH})\text{L}_2]^+ / [\text{CuL}_2]$ (each

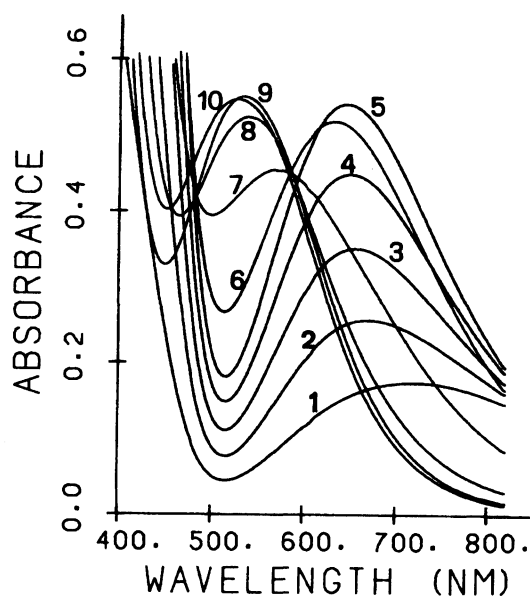


Fig. 3. Plots of experimental absorbance data versus wavelength for solutions [C_L range 9.937×10^{-3} — 1.267×10^{-2} mol dm $^{-3}$, C_M range 4.977×10^{-3} — 6.548×10^{-3} mol dm $^{-3}$; (1) pH=3.478, (2) pH=3.577, (3) pH=3.680, (4) pH=3.817, (5) pH=4.104, (6) pH=5.116, (7) pH=5.640, (8) pH=6.110, (9) pH=7.557, (10) pH=9.790] of Cu $^{2+}$ -ahmpe1 system at 25°C using the program VISION with the Plotter Calcomp 936.

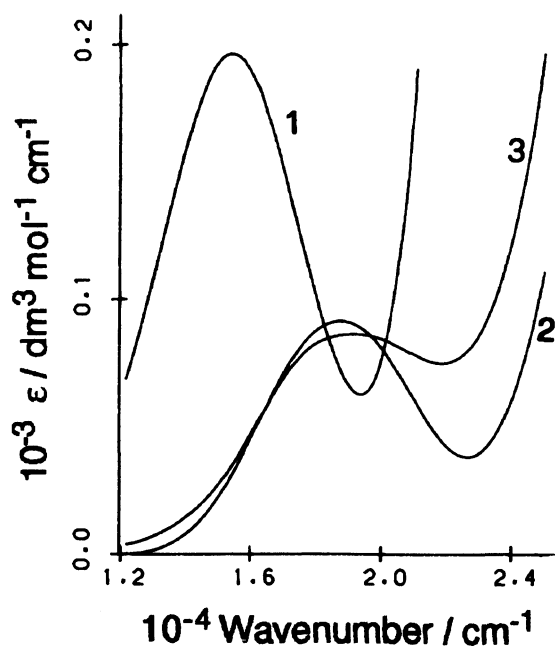


Fig. 4. Plots of molar extinction coefficients (ϵ) of the three complexed species of Cu $^{2+}$ -ahmpe1 system: (1) ϵ [Cu $_2$ (OH)L $_2$] $^{+}$; (2) ϵ [CuL $_2$ (H $_2$ O) $_2$]; (3) ϵ [Cu(OH)L $_2$] $^{-}$.

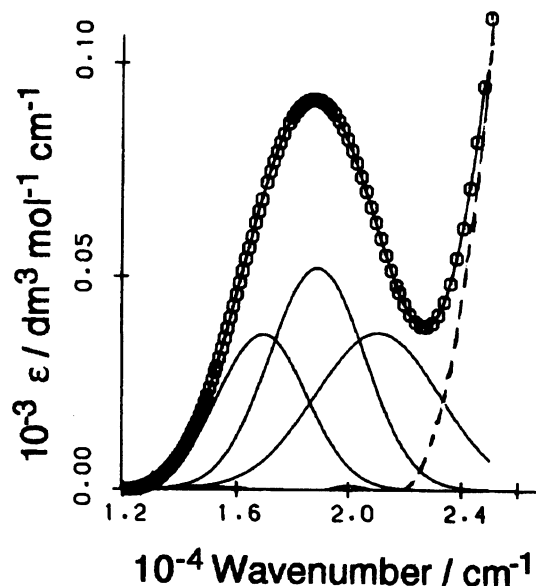


Fig. 5. Absorption spectra of [CuL $_2$ (H $_2$ O) $_2$]: experimental (symbol) and calculated (line); (—) composite bands; (---) unassigned band.

species is present for the 49.3% total copper at pH 5.35, [Fig. 2]. For a comparison of the spectrophotometric properties of these complexes with those formed by other analogous amino hydroxamic acids seen reports of Table 3. The molar absorption coefficients ϵ_{pqr} in the range 400–820 nm for the Cu $^{2+}$ -ahmpe1 system (all the formation constants already refined were kept constant) were determined by handling the specific sets of absorbance data (14 solutions, 211 wavelengths, 2954 experimental absorbance points) by using the SQUAD¹³) program (Fig. 4). The standard deviation in the absorbance data of 14 solutions and 211 wavelengths was 2.797×10^{-2} , suggesting that the fit of the calculated spectra to the observed ones is very good. In order to interpret the [CuL $_2$ (H $_2$ O) $_2$] spectrum, a careful and detailed Gaussian analysis of the experimental data (Fig. 4, curve 2, 211 experimental data points) was carried out by using a NLIN computer program (SAS Institute Inc., SAS/STAT Users Guide: Version 6 *Fourth Edition*, Volume 2, Cary, NC. SAS Institut Inc., 1989, p. 1135). Moreover the Gaussian analyses, based on the nonlinear Marquardt least-squares method which allowed O_h (one band) and D_{4h} (three bands) symmetry, were different in terms of the relative standard deviation. Finally, starting from the maximum positions (ν) of the precisely positioned component bands (Fig. 5), the ligand-field parameters, D_q , D_s , and D_t , which were consistent with the effective D_{4h} symmetry of the ligand donor atoms in a hexa-coordinate geometry (tetragonally distorted) about the copper ion, were calculated. In this case the term B_{1g} will be ground state and three-spin allowed transitions from the $^2B_{1g}$ state to the other doublet states expected. The relative energy order of these transitions ($^2A_{1g} < ^2B_{2g} < E_g$) will depend

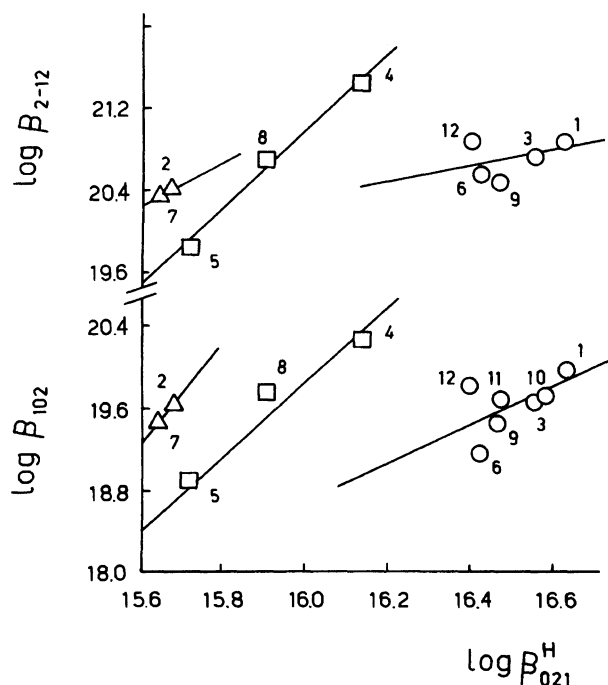


Fig. 6. Correlation between cumulative protonation constant $\log \beta_{021}$ of different amino hydroxamic acids and stability constants ($\log \beta_{102}$, $\log \beta_{2-12}$) of their copper(II) chelates. (1) ahpr=2-amino-*N*-hydroxypropanamide, Ref. 11; (2) adhp=2-amino-*N*,3-dihydroxypropanamide, Ref. 21; (3) ahhe=2-amino-*N*-hydroxyhexanamide; (4) ahnp= α -amino-*N*-hydroxy-1*H*-indole-3-propanamide; (5) aimahp=2-amino-5-[(aminoiminomethyl)amino]-*N*-hydroxypentanamide, Ref. 19; (6) ahmpe=2-amino-*N*-hydroxy-4-methylpentanamide, Ref. 15; (7) adhb=2-amino-*N*,3-dihydroxybutanamide, Ref. 20; (8) ahpp=2-amino-*N*-hydroxy-3-phenylpropanamide; (9) ahbt=DL-2-amino-*N*-hydroxybutanamide, Ref. 22; (10) aha=2-amino-*N*-hydroxyacetamide; (11) ahp=2-amino-*N*-hydroxypentanamide; (12) ahmpe1=2-amino-*N*-hydroxy-3-methylpentanamide (present work).

on the axial metal-water interaction and their energies in terms of the parameters D_q , D_s , and D_t have been obtained from the expressions: $\nu_1 = -4D_s - 5D_t$; $\nu_2 = 10D_q$; $\nu_3 = 10D_q - 3D_s + 5D_t$ ($D_q = \nu_2/10 = 1893.9$; $D_s = 1/7[\nu_2 - \nu_1 - \nu_3] = -2719.4$; $D_t = 1/35[4(\nu_3 - \nu_2) - 3\nu_1] = -1209.8$). From the results obtained in the present work (ν , $\Delta\nu$, ε , $f = 4.6 \times 10^{-9} \varepsilon_{\max} \Delta\nu$) relating to the components bands, it is possible to verify an excellent agreement between the parameters calculated for the different systems (see results reported in Table 3), thus suggesting that a similar trend (structure, configuration, thermodynamic stability) is displayed in the course of $[\text{CuL}_2(\text{H}_2\text{O})_2]$ complex formation. However, the small differences observed in the parameters D_s and D_t for the different systems mean that the energies for a tetragonal distortion, commonly given in terms of the radial parameters,

are slightly different for $[\text{CuL}_2(\text{H}_2\text{O})_2]$ complex. In general the complexes of Co^{2+} and Ni^{2+} exhibit similar behavior to those of Cu^{2+} , but the later have higher stabilities as expected. Moreover the small difference in the structure of the internal coordination sphere of copper (II) chelates (as observed in the spectrophotometric properties, see results of Table 3) as $[\text{Cu}_2(\text{OH})\text{L}_2]^+$ and $[\text{CuL}_2(\text{H}_2\text{O})_2]$ for the different amino hydroxamic acids is also manifested by a correlation between the $\log \beta_{021}^H$ values of individual ligands and the values of stability constants ($\log \beta_{2-12}$, $\log \beta_{102}$) of appropriate copper(II) chelates formed after the dissociation of two protons from $-\text{NH}_3^+$ and $-\text{CONHOH}$ group-coordinated. The Jones's correlation equation²³⁾ $\log \beta_{pqr} = a \log \beta_{021}^H + b$ (where a and b are constants and β_{pqr} is the stability constant) was applied to the examined group of copper(II) chelates. It was found that satisfactory correlation holds for the chelates of the different ligands into three groups: (1) with aliphatic chain (○), 1, 3, 6, 9, 10, 11, and 12; (2) with hydroxy group on the chain (△), 2 and 7; (3) with conjugated moiety (aromatic or aminoiminomethyl group, etc.) on the chain (□), 4, 5, and 8 (see Fig. 6). The linear free energy relationship between protonation constant and stability constant holds for each group of ligands independently. This fact reflects in a different structure of the ligands, in which the introduction of various groups (as indolyl, aminoiminomethyl, hydroxy, etc.) into the molecule resulted in a significant variation of the basicity of the functional groups ($-\text{NH}_2$, $-\text{CONHO}^-$) besides sterical reasons not always followed by similar difference in the stability of the coordination sphere. Three parallel lines are obtained, with almost similar slopes and different intercepts, and thus the latter indicating the characteristics of the class of ligands.

The Cu^{2+} -ahmpe1 system probably satisfies different criteria for biological activities and analytical roles, strongly indicating Cu^{2+} -ahmpe1 complexes as suitable sources of copper as trace element essential in animal nutrition.

Grateful acknowledgement is made to the Ministero dell'Università e della Ricerca Scientifica e Tecnologica (M.U.R.S.T.) and National Research Council of Italy (C.N.R.) for generous grants. I am greatly indebted to Professors P. Gans, A. Vacca, and A. Sabatini for their generous support of the program SUPERQUAD.

References

- 1) H. Kehl, "Chemistry and Biology of Hydroxamic Acids," Karger, New York (1982).
- 2) H. Maehr, *Pure Appl. Chem.*, **28**, 603 (1971).
- 3) J. C. Powers and J. W. Harper, in "Proteinase Inhibitors," ed by A. J. Barrett and G. Salvesen, Elsevier, Amsterdam (1986), p. 244.
- 4) Y. K. Agrawal, *Bull. Soc. Chim. Belg.*, **89**, 166 (1980).

- 5) E. Leporati, *J. Chem. Soc., Dalton Trans.*, **1986**, 2587.
 - 6) E. Leporati, *J. Chem. Soc., Dalton Trans.*, **1987**, 435.
 - 7) E. Leporati, *J. Chem. Soc., Dalton Trans.*, **1987**, 1409.
 - 8) G. Gran, *Analyst (London)*, **77**, 661 (1952).
 - 9) H. S. Harris and R. S. Tobias, *Inorg. Chem.*, **8**, 2259 (1969).
 - 10) D. J. Leggett, "Computational Method for the Determination of Formation Constants," Plenum, New York and London (1987), p. 37.
 - 11) E. Leporati, *J. Chem. Soc., Dalton Trans.*, **1989**, 1299.
 - 12) P. Gans, A. Sabatini, and A. Vacca, *J. Chem. Soc., Dalton Trans.*, **1985**, 1195.
 - 13) D. J. Leggett and W. A. E. McBryde, *Anal. Chem.*, **47**, 1065 (1975).
 - 14) E. Leporati, *J. Chem. Soc., Dalton Trans.*, **1988**, 421.
 - 15) E. Leporati and G. Nardi, *Bull. Chem. Soc. Jpn.*, **64**, 2488 (1991).
 - 16) B. Kurzak, K. Kurzak, and J. Jezierska, *Inorg. Chim. Acta*, **125**, 77 (1986).
 - 17) E. B. Paniago and S. Carvalho, *Inorg. Chim. Acta*, **92**, 253 (1984).
 - 18) B. Kurzak, K. Kurzak, and J. Jezierska, *Inorg. Chim. Acta*, **130**, 189 (1987).
 - 19) E. Leporati and G. Nardi, *Gazz. Chim. Ital.*, **121**, 147 (1991).
 - 20) E. Leporati, *Inorg. Chem.*, **28**, 3752 (1989).
 - 21) E. Leporati, *Gazz. Chim. Ital.*, **119**, 183 (1989).
 - 22) E. Leporati, *J. Chem. Res. (S)*, **1990**, 14.
 - 23) J. G. Jones, J. B. Poole, J. C. Tomkinson, and R. J. P. Williams, *J. Chem. Soc.*, **1958**, 2001.
-